Shalitin, N., & Feitelson, J. (1976b) in *Excited States of Biological Molecules* (Birks, J. B., Ed.) pp 190–198, Wiley-Interscience, New York.
Siegel, S., & Goldstein, L. (1965) *J. Chem. Phys. 43*, 4185–4187.
Singhal, R. P., & Fallis, P. A. M. (1979) *Progr. Nucleic Acid Res. Mol. Biol. 23*, 227–290.
Sprinzl, M., Grüter, F., & Gauss, D. H. (1978) *Nucleic Acids Res. 5*, r15–r27.
Steiner, R. F., Miller, D. B., & Heerman, K. C. (1967) *Arch. Biochem. Biophys. 120*, 464–467.
Taherian, M.-R., & Maki, A. H. (1981) *Chem. Phys. 55*, 85–96.
Teeter, M. M., Quigley, G. J., & Rich, A. (1980) in *Nucleic Acid-Metal Ion Interactions* (Spiro, T. G., Ed.) pp 145–177, Wiley-Interscience, New York.
Walker, R. T., & RajBhandary, U. L. (1970) *Biochem. Biophys. Res Commun. 38*, 907–914.
Winscom, C. J., & Maki, A. H. (1971) *Chem. Phys. Lett. 12*, 264–268.
Wong, K. L., & Kearns, D. R. (1974) *Nature (London) 252*, 738–739.
Wong, K. L., Bolton, P. H., & Kearns, D. R. (1975) *Biochim. Biophys. Acta 383*, 446–451.
Yaniv, M., & Barrell, B. G. (1969) *Nature (London) 222*, 278–279.
Zuclich, J., von Schütz, J. U., & Maki, A. H. (1974) *J. Am. Chem. Soc. 96*, 710–714.

Secondary Structure of Prokaryotic 5S Ribosomal Ribonucleic Acids: A Study with Ribonucleases†

Steve Douthwaite and Roger A. Garrett*

ABSTRACT: The structures of 5S ribosomal RNAs from *Escherichia coli* and *Bacillus stearothermophilus* were examined by using ribonucleases A, T_1, and T_2 and a double helix specific cobra venom ribonuclease. By using both 5′- and 3′-^{32}P-end labeling methods and selecting for digested but intact 5S RNA molecules, we were able to distinguish between primary and secondary cutting positions and also to establish the relative degree of cutting. The data reveal the predicted similarities of the higher order structure in the two RNAs but also demonstrate a few significant differences. The data also provide direct evidence for three of the helical regions of the Fox and Woese model of 5S RNA [Fox, G. E., & Woese, C. (1975) *Nature (London) 256*, 505] and support other important structural features which include a nucleotide looped out from a helical region which has been proposed as a recognition site for protein L18.

5S RNA is the smallest ribosomal RNA and is an integral part of the large ribosomal subunit. Although its function in protein biosynthesis remains unknown, it has been located by immunoelectron microscopy and reconstitution experiments in a region of the 50S subunit interface known to be associated with peptidyltransferase activity (Stöffler et al., 1980; Dohme & Nierhaus, 1976). The relative structural simplicity of 5S RNA has rendered it an obvious choice for studies on both ribosomal RNA secondary structure and the chemistry and specificity of protein–RNA interactions. A base-pairing scheme common to all prokaryotic 5S RNAs, consisting of four double-helical regions, was first proposed by Fox & Woese (1975) on the basis of comparative sequence studies. This almost certainly constitutes the minimum amount of base pairing in the 5S RNA since several lines of evidence indicate that the remainder of the RNA is also highly structured. For example, only 4 out of the remaining 21 "unpaired" guanines in the *Escherichia coli* RNA structure are strongly modified by kethoxal (Noller & Garrett, 1979) and a large region (nucleotides 69–87 and 89–110) is highly resistant to ribonuclease A (Douthwaite et al., 1979).

The object of the present study was to exploit the new rapid RNA gel sequencing technology to investigate the topography of the A form of 5S RNA by using ribonucleases of different specificities. Ribonucleases A, T_1, and T_2 have a strong preference for single-stranded regions, and the *Naja naja oxiana* cobra venom ribonuclease is specific for double-helical structures (Vassilenko & Babkina, 1965).

In earlier studies with ribonucleases A, T_1, and T_2, cutting positions have generally been assumed to occur in accessible, non-base-paired regions (Monier, 1974). However, this interpretation is subject to the criticism that a primary cut may produce a structural rearrangement which results in a secondary cut occurring at a position which is not accessible in the native structure. In the present study, we have tried to overcome this problem first by performing very mild digests and then selecting, electrophoretically, for intact 5S RNA molecules with a few nicks. Second, we have employed both 3′- and 5′-end-labeled RNA which generally enables us to distinguish between primary and secondary cuts. We have then analyzed the positions and intensities of the cuts over a range of enzyme conditions, on rapid sequencing gels. The structures of two ribosomal 5S RNAs, from *E. coli* and *Bacillus stearothermophilus*, were examined and special attention was given to common features. A fairly detailed picture emerges of the RNA structure; the data provide experimental support for the base-pairing scheme of Fox & Woese (1975) and yield further insight into the structure of the other RNA regions.

Materials and Methods

5S RNA was isolated from *E. coli* strain MRE 600 and *B. stearothermophilus* strain NCA 1503, following the general

† From the Division of Biostructural Chemistry, Kemisk Institut, Aarhus Universitet, DK-8000 Aarhus C, Denmark. *Received June 4, 1981*. This work was supported by a temporary research grant from the Danish Research Council. S.D. gratefully received support from Aarhus University, the Deutsche Forschungsgemeinschaft, the Max-Planck-Institut für Molekulare Genetik in West Berlin, and EMBO.

0006-2960/81/0420-7301$01.25/0

procedure of Monier & Feunteun (1971). The RNA was 5′-end labeled. It was first dephosphorylated with alkaline phosphatase (Boehringer-Mannheim) at 55 °C for 30 min. It was then purified on a 12% polyacrylamide slab gel (20 × 20 × 0.2 cm) containing 50 mM Tris–borate, pH 8.3, 1 mM EDTA, and 8 M urea and run at 30 V/cm for 1.5 h. RNA was extracted from the gel with 0.24 M NH_4 acetate, pH 5, and an equal volume of phenol saturated in buffer and precipitated with ethanol before reacting with [γ-^{32}P]ATP (Amersham) and T_4 polynucleotide kinase (P-L Biochemicals). 3′-End labeling was attained with [^{32}P]Cp (Amersham) and RNA ligase (P-L Biochemicals) as described by Peattie (1979).

The RNA was renatured by dissolving in 10 mM Tris-HCl, pH 7.8, 0.5 mM $MgCl_2$, and 40 mM KCl at 70 °C for 5 min and slowly cooled to 35 °C, before placing on ice (Weidner & Crothers, 1977). RNA was digested with ribonucleases A (Sigma) and T_1 and T_2 (Sankyo) and *N. naja oxiana* cobra venom ribonuclease (gift of S. Vassilenko) in TMK buffer (30 mM Tris-HCl, pH 7.8, 20 mM $MgCl_2$, 300 mM KCl) at increasing ribonuclease/RNA ratios at 0 °C. The concentration ranges used were 1:5000 to 1:500 units per μg of RNA for RNase T_1, 1:5000 to 1:50 units per μg of RNA for RNase T_2, 1:10 000 to 1:50 units per μg of RNA for RNase A, and 1:300 to 1:100 units per μg of RNA for the cobra venom ribonuclease. The digested samples were electrophoresed in 12% polyacrylamide gels (20 × 20 x 0.2 cm) containing 40 mM Tris-HCl and 10 mM $MgCl_2$, pH 8, at 4 °C and about 7 v/cm for 16 h. The buffer was circulated. The band migrating alongside undigested 5S RNA was detected by autoradiography and excised. A few fragments which migrated faster than the 5S RNA were also examined for their enzyme cuts. RNA was extracted from the gel in 0.2 M ammonium acetate, pH 5.5; for the RNase T_2 treated sample, an equal volume of phenol was also employed in the extraction to remove the ribonuclease which coelectrophoreses with the 5S RNA. The RNA was precipitated with 2.5 volumes of ethanol, washed with ethanol, and dried.

Twelve percent polyacrylamide sequencing gels (40 × 40 × 0.04 cm) were prepared as described earlier (Peattie, 1979). 5S RNA was subjected to base-specific chemical modification following the procedure of Peattie (1979). All samples were dissolved in loading buffer and coelectrophoresed with the ribonuclease-treated samples at 50 W. For the 5′-labeled samples, a reference ladder was generated by boiling a sample in loading buffer for 45 min. Gels were autoradiographed, and both the nucleotide sequence and the positions and intensities of ribonuclease cuts were deduced from the films.

Results

Isolation and Analysis of Digested 5S RNA. 5S RNA from *Escherichia coli* or *B. stearothermophilus* labeled at their 5′ or 3′ ends was renatured and dissolved in ribosomal TMK buffer. The RNA was treated with increasing concentrations of ribonucleases A, T_1, or T_2 or cobra venom ribonuclease at 0 °C and subsequently electrophoresed in a 12% polyacrylamide gel containing 10 mM magnesium in order to purify the digested but intact 5S RNA molecules from the smaller breakdown products. An example is shown in Figure 1 for a range of ribonuclease A concentrations. The RNA which comigrated with undigested 5S RNA (position I) was extracted from the gel, denatured by heating in 8 M urea, and run in an RNA sequencing gel alongside 5S RNA samples which had been subjected to the chemical sequencing procedure of Peattie (1979). In this way, the positions and intensities of the RNA cuts could be determined. In general, a range of enzyme conditions was tested in order to investigate the progressive disruption of the RNA structure. The results obtained for each of the ribonucleases, with both *E. coli* and *B. stearothermophilus* 5S RNAs, are presented in Tables I–IV and the data are summarized in Figures 4 and 5.

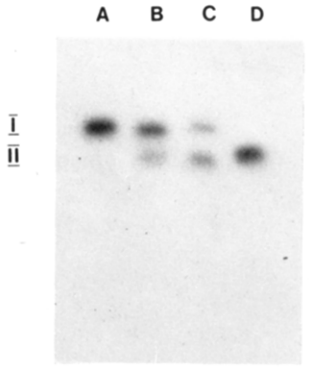

FIGURE 1: Purification of 3′-Labeled *E. coli* 5S RNA after ribonuclease A treatment. (A) Undigested sample. (B, C, and D) Treated at ribonuclease A:RNA ratios of 1:1000, 1:500, and 1:50 w/w, respectively, for 10 min at 0 °C in TMK buffer before loading on a 12% polyacrylamide gel containing 40 mM Tris-HCl and 10 mM $MgCl_2$, pH 8.0, and electrophoresing overnight. I indicates the position of the 5S RNA, and II corresponds to fragmented RNA.

In the latter figures the secondary structure is based on the model of Fox & Woese (1975) with four helices numbered I–IV. For the *E. coli* RNA they constitute the respective sequences 1–10/110–120, 18–23/60–65, 31–34/48–51, and 82–86/90–94. The models presented contain additional base pairing which extends helices II and IV and structures the region between helices II and III; these refinements are considered later.

Definition of Primary and Secondary Cuts. A distinction is generally made between primary and secondary cuts. We define the former as those which occur in the intact 5S RNA molecule and can be seen in both 5′- and 3′-labeled samples on sequencing gels. We infer that a primary cut occurs at an accessible nucleotide. A secondary cut is defined as occurring as a result of, and subsequent to, a primary cut. It is seen in either a 5′ or 3′-labeled sample, but not in both, and it occurs at an inaccessible or partially inaccessible nucleotide. For example, as illustrated in Figure 2, when the 3′-labeled sample of *B. stearothermophilus* 5S RNA was digested with ribonuclease T_2, it yielded a strong band at C_{39} and no cuts at C_{36} to U_{38} (Figure 2A, lane 2), whereas the 5′-end labeled sample, treated in the same way, produced strong cuts at C_{39} and additional cuts at C_{36} to U_{38} (Figure 2B, lane 1). By our definition, the cut at C_{39} is primary, whereas those at C_{36} to U_{38} are secondary.

Quantitation of Ribonuclease Cuts. It is very difficult to attain any precise quantitation of cuts for two main reasons. First, when a very strong cut occurs in the molecule, as is often the case (see Figures 2 and 3), the cuts beyond that position (away from the end label) are necessarily weak. This complication can be overcome partially by examining both 5′- and 3′-labeled molecules, but it can still lead to difficulties when, for example, a weaker cut occurs between two especially strong cuts. The other reason is that secondary cutting may influence the quantitation of primary cuts. Although most secondary cuts are weak and exhibit relatively slow kinetics, a few occur more rapidly than some primary cuts: for example, the ribonuclease T_2 cut at A_{53} in the *E. coli* 5S RNA occurs in rapid succession to the primary cut at A_{52} (see Tables I and III). Such secondary cutting may then destabilize the RNA structure and enhance weaker primary cuts. Therefore, we

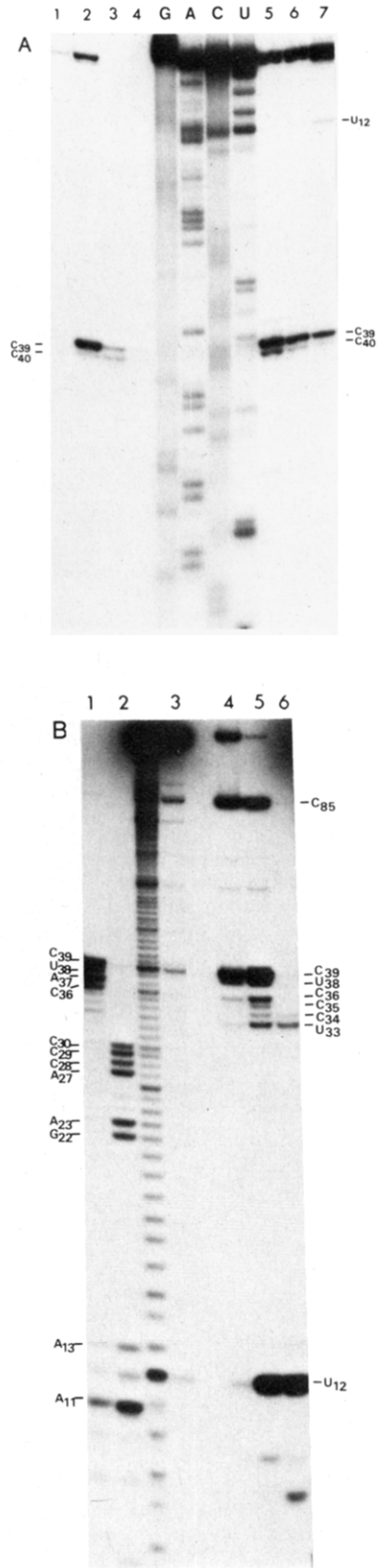

FIGURE 2: *B. stearothermophilus* 5S RNA treated with ribonucleases A and T_2. (A) 3′-Labeled 5S RNA: lane 1, undigested sample; lanes 2, 3, and 4, digestion with ribonuclease T_2 at 1:1000, 1:100, and 1:50 units/μg of RNA, respectively, for 30 min at 0 °C; lanes 5, 6, and 7, treatment with ribonuclease A at 1:10000, 1:5000, and 1:1000 w/w, respectively, for 10 min at 0 °C. The central samples were chemically sequenced for the four nucleotides. (B) 5′-Labeled 5S RNA: lane 1, digestion with ribonuclease T_2 at 1:50 units/μg of RNA; lane 2, an RNA fragment which comigrated with the sample in lane 1 on a purification gel; lane 3, undigested sample; lanes 4, 5, and 6, digestion with ribonuclease A at 1:10000, 1:1000, and 1:100 w/w, respectively. The central ladder was produced by boiling the RNA in loading buffer.

Table I: Primary Ribonuclease Cuts Occurring in the A Form of *E. coli* 5S RNA

	ribonuclease			
nucleotide	A	T_1	T_2	cobra venom
C_{12}	+		+	
G_{13}		+	+	
U_{14}	++			
G_{20}				++
C_{35}	+		+	
C_{38} [a]	++		+	
U_{40}	(+)		+	
G_{41}		+++	+++	
C_{42}	+++		+S [b]	
A_{52}			++	
C_{63}				++
G_{64}				++
U_{65}	++			
G_{81}				+
G_{86}		++		
U_{87}	++		(+)	
C_{88}	++		+	
U_{89}	++		(+)	
C_{93}				+
G_{114}				+++

[a] It is uncertain whether this constitutes a primary or secondary cut; it is not included in Figure 4. [b] S indicates that this is a secondary cut with ribonuclease T_2.

have kept to a relatively crude (+) system which has been compiled by examining visually many autoradiograms of both 5′- and 3′-labeled samples.

Identification of Primary Cuts. (*a*) *E. coli.* Three very accessible unstructured regions occur around nucleotides C_{12} to U_{14}, U_{40} to C_{42}, and G_{86} to U_{89}. Primary cuts occur at each of these nucleotides drawn in loops in Figure 4. Additional cuts adjacent to these regions are secondary and occur as a result of prior opening in this region (see below). Other very accessible nucleotides which have not been described previously occur after A_{52} (ribonuclease T_2) and after C_{35}, C_{38} (see later comment), and U_{65} (ribonuclease A). We could find no evidence that these accessible regions extend beyond one base, although a strong secondary cut is seen after A_{53} (see below).

The cobra venom ribonuclease cuts occur exclusively in the double helices of the Fox & Woese (1975) model. The results which are presented in Table I support helices I, II, and IV of this model. Two cuts occur on only one side of the helix. The other cuts appear on opposite sides of the helix. No cut is observed in helix III, the shortest of the helices (Figure 4). Somewhat surprisingly, no cuts were observed on the 5′ side of helix I, in either 3′- or 5′-labeled samples. In order to ensure that a small 5′-labeled fragment had not dissociated during the purification gel, after 5S RNA digestion, a 5′-labeled sample was digested and run directly on a sequencing gel without further purification, as shown in Figure 3 for the *B. stearothermophilus* 5S RNA. No small 5′-labeled fragment was detected. All of the cobra venom ribonuclease cuts were detected in both 5′- and 3′-labeled samples, confirming their primary nature. The 5′-labeled samples migrated slightly slower than the water-hydrolyzed samples, suggesting that the 3′-phosphate is excised by the ribonuclease. This mobility difference can be used to advantage since there is no difficulty in distinguishing the cobra venom ribonuclease cuts from any which may be present in the 5S RNA control sample.

(*b*) *B. stearothermophilus.* Differences occur among the published nucleotide sequences for *B. stearothermophilus* 5S RNA, so we first sequenced strain NCA 1503 using Peattie's (1979) procedure. The sequencing tracks are illustrated in Figure 2A. We obtained the same result as Stanley & Pen-

Table II: Primary Ribonuclease Cuts Occurring in *B. stearothermophilus* 5S RNA

nucleotide	ribonuclease A	T_1	T_2	cobra venom
G_{10}		+		
A_{11}			+	
U_{12}	+			
A_{13}			+	
G_{14}		(+)		
G_{16}				+
A_{18}				++
G_{19}				+
G_{21}				++
G_{22}				+
A_{27}				+
C_{28}				+
C_{30}				+
U_{38}	+		+S[b]	
C_{39}	+++		++	
C_{40}	++		+	
G_{42}		(+)		
A_{50}			(+)	+
G_{52}		(+)		
U_{54}				(+)
C_{59}				++
C_{60}				++
U_{61}				++
G_{65}		(+)		
G_{67}		(+)		
U_{79}				+++
G_{80}				++
C_{85}	++			
A_{86}[a]	+S[b]		++	
G_{87}		+++	+	
C_{92}				+
C_{93}				+
U_{110}				+
G_{111}				+++
C_{112}				++
U_{113}				+

[a] There appears to be a sequence heterogeneity at this position; an enhanced U band was discernible on some sequencing gels. [b] S indicates that it was a secondary cut with certain enzymes.

swick (1975) which is drawn in Figure 5.

Three very accessible single-stranded regions were observed, as for *E. coli*, at G_{10} to A_{13}, U_{38} to C_{40}, and C_{85} to G_{87}. Secondary cuts were detected adjacent to these regions (see Table IV). No other strong primary cuts were observed in the RNA, although very weak cuts were observed with T_1 ribonuclease at G_{14}, G_{42}, G_{52}, G_{65}, and G_{67} (Table II).

More extensive cobra venom ribonuclease cutting was observed than for the *E. coli* 5S RNA, and this was reflected in the relatively easy fragmentation of the *B. stearothermophilus* RNA. In particular, the stem region was readily excised due, partly, to strong cuts in the U_{110} to U_{113} region. Nevertheless, strong cobra venom ribonuclease cuts occurred at positions within helices I, II, and IV corresponding to those of the *E. coli* RNA. The cuts at G_{21}, U_{79}, and G_{80} (Figure 3) could only be assigned unambiguously in the 5′-labeled samples because strong compression of the ladder of the 3′-labeled sample occurred at these positions due to the high G content of the terminal sequences.

A weak cut was observed in helix III at C_{30} (see Figure 3). Additional weak cuts were also observed at G_{22}, A_{27}, C_{28}, A_{50}, and U_{54} in the region between helices II and III. These are indicated in the structure for this interhelical region proposed recently by Studnicka et al. (1981) which is drawn in Figure 5. However, three of the five cuts at positions G_{22}, A_{50}, and U_{54} do not occur directly in the proposed helix; they occur in the looped out regions.

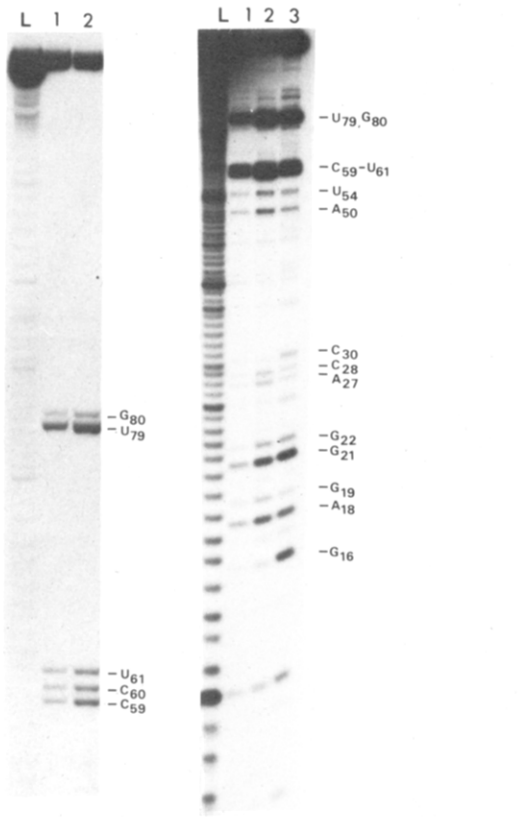

FIGURE 3: 5′-Labeled *B. stearothermophilus* 5S RNA treated with cobra venom ribonuclease. Samples were digested at 1:100 units/μg of RNA at 0 °C for 30 min (lane 1) and for 60 min (lanes 2 and 3). The 5S RNA in lane 3 was not purified on a polyacrylamide gel after digestion. The positions of the cuts are indicated. The ladder was produced as described for Figure 2B.

Table III: Secondary Ribonuclease Cuts Occurring in the A Form of the *E. coli* 5S RNA

nucleotide	ribonuclease	degree of cut	end labeling	dependent on primary cut
C_{17}	A	+	3′	U_{14}
C_{36}	A	+	5′	C_{38}
C_{37}	A	+	5′	C_{38}
A_{39}	T_2	++	5′	U_{40}
C_{42}	T_2	+	3′	G_{41}
C_{43}	A/T_2	+++/+	3′	C_{42}/G_{41}
G_{44}	T_1/T_2	++	3′	G_{41}
C_{47}	A	+	3′	C_{42}
C_{49}	A	(+)	3′	C_{42}
A_{53}	T_2	++	3′	A_{52}
U_{55}	A	(+)	3′	
C_{68}	A	++	3′	U_{65}

Table IV: Secondary Ribonuclease Cuts Occurring in the *B. stearothermophilus* 5S RNA

nucleotide	ribonuclease	degree of cut	end labeling	dependent on primary cut
U_{33}	A/T_2	++/+	5′	C_{39}
C_{34}	A/T_2	+	5′	C_{39}
C_{35}	A/T_2	+	5′	C_{39}
C_{36}	A/T_2	+	5′	C_{39}
A_{37}	T_2	++	5′	C_{39}
U_{38}	T_2	++	5′	C_{39}
A_{86}	A	+	3′	C_{85}
C_{88}	T_2	+	3′	C_{85}

Identification of Secondary Cuts. These results are listed in Tables III and IV for the *E. coli* and *B. stearothermophilus* 5S RNAs, respectively. The secondary cuts were only observed for the single-strand-specific ribonucleases. Whether the cut

was detected exclusively in the 5′- or 3′-labeled sample is indicated; this determines on which side of the primary cut the secondary cut falls. Most of the latter occurred adjacent to accessible regions and could generally be correlated with a primary cut (See Tables III and IV).

The secondary cuts presented are still a selection, however, in the sense that they do not cause gross disruption and fragmentation of the 5S RNA structure. The latter cuts will only be found in fragments and they are considered briefly below.

RNA Fragments. The strategy of the present study was to investigate the cuts in those 5S RNA molecules which are not fragmented, and therefore, no comprehensive study was made of RNA fragments. Nevertheless, a few fragments were examined which bear some relevance to the present structural studies.

Fragments observed in 5′-labeled samples of both RNAs revealed the opening of helix III and the adjacent region between helices II and III (Figures 4 and 5). A fragment of *E. coli* 5S RNA, produced with ribonuclease A, exhibited cuts at U_{25} to C_{28} and C_{30}, whereas a ribonuclease T_2 fragment of *B. stearothermophilus* RNA contained cuts at G_{22}, A_{23}, and A_{27} to C_{30}. These data suggest a cooperative opening effect in this region because the intensities of the bands were approximately equal. Since no cuts occur on the opposite side of the helix which could trigger such cooperative destructuring, it seems probable that the destabilizing effect derives from progressive digestion, in a 5′ direction from around nucleotide 40.

A further fragment having some bearing on the proposed structure was produced from the *B. stearothermophilus* RNA with cobra venom ribonuclease. It showed a series of cuts extending up the 3′ side of helix IV at each of the residues C_{91} to A_{97}, a region which was relatively inaccessible in the intact 5S RNA. This observation lends support to the proposed extension of helix IV drawn in Figures 4 and 5 (Noller & Garrett, 1979).

Methodological Limitations. There were a number of limitations to the method. The interpretation of the sequencing gels was sometimes complicated for 5′- and 3′-labeled samples. For both bacterial RNAs, high concentrations of ribonuclease A removed the Cp of the [^{32}P]Cp 3′-labeled samples, resulting in doublet bands. In addition, the 3′-uridine of the *E. coli* 5S RNA was sometimes present in submolar amounts which also led to double-band formation of 3′-labeled samples. Finally, the 5′-labeled samples of *E. coli* yielded doublet and occassionally triplet bands, possibly due to the loss of a 3′-phosphate, or formation of a cyclic phosphate at the 3′ end. These results did not impair the interpretation of the films, but it was necessary to compare carefully the results for both 5′- and 3′-labeled samples to avoid mistakes.

There is a possible ambiguity in the assignment of primary cuts; if a secondary cut, at a given position, can be caused by a primary cut on both its 5′ and 3′ sides, by our criterion it could be incorrectly assigned as a primary cut. To some extent we have covered this for the non-double-helical regions by using three single-strand-specific nucleases with different but overlapping nucleotide specificities. However, the assignment of the ribonuclease cut at C_{38}, in the *E. coli* 5S RNA, is ambiguous, since it could be a primary cut or it could be secondary to both neighboring primary cuts on its 5′ and 3′ sides (see Table I and Figure 4).

There is some uncertainty as to whether some of the very weak cuts are primary or secondary. In general, it would require long exposure of gels of both 5′- and 3′-labeled samples

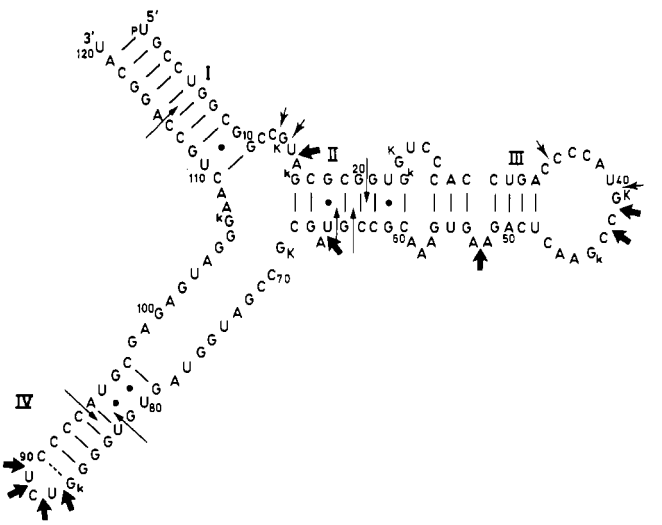

FIGURE 4: *E. coli* 5S RNA drawn according to the Fox and Woese secondary structural model with extensions to helices II and IV as described in the text. The arrows mark the primary cutting positions of ribonucleases A, T_1, and T_2 which show a strong preference for single-stranded regions: large arrows correspond to strong cuts and small arrows indicate weak cuts. Secondary cutting positions are not shown. If a nucleotide is cut strongly by one ribonuclease and weakly by another, the cut is represented with a large arrow. Arrows drawn into the helices and across the polynucleotide chain represent the sites of the cobra venom ribonuclease cuts; again the arrow size defines the degree of cutting. Further details of the enzyme cuts are given in Tables I–IV. The kethoxal-reactive guanines are also indicated by large and small K's, according to the relative rate of modification, as determined by Noller & Garrett (1979).

to be sure of this. However, there is also the possibility that very weak cuts which occur in both 5′- and 3′-labeled samples and are designated primary are attributable to other conformers. The *E. coli* 5S RNA is known to exist in two major conformational forms, the A and B forms, and although the RNA was renatured so as to produce the A form and any remaining B form should have been removed during the gel purification step, we cannot eliminate the possibility that traces of the B form or other conformers are present. This leaves some uncertainty, therefore, in defining very weak primary cuts.

In general, a few weak bands were present in the undigested control samples (see, for example, Figure 2 and 3). These effects were not eliminated by further purification on urea–polyacrylamide gels, and we concluded that they were caused by radiolytic damage. The problem was worse for highly radioactive samples and after longer storage times; moreover, the cuts occurred predominantly at U–A bonds, in particular at the U_{103}–A_{104} bond in *E. coli* 5S RNA which was not cut by the ribonucleases.

Discussion

The secondary structural model used in the present work and illustrated in Figures 4 and 5 is modified from that of Fox & Woese (1975). Helix II is extended by two base pairs, G_{16}–C_{68} and C_{17}–G_{67} in the *E. coli* RNA and a looped out adenine, which are supported by comparative sequence studies (Peattie et al., 1981; Garrett et al., 1981; Studnicka et al., 1981). The region between helices II and III is drawn with three additional base pairs, as were drawn in numerous earlier models of *E. coli* RNA (Erdmann, 1976); recently, Studnicka et al. (1981) have proposed three base pairs in a slightly different configuration for Gram-positive bacteria (Figure 5). The relatively unstable extension to helix IV of base pairs U_{95}–G_{81}, G_{96}–U_{80}, and C_{97}–G_{79} in *E. coli* 5S RNA (Noller

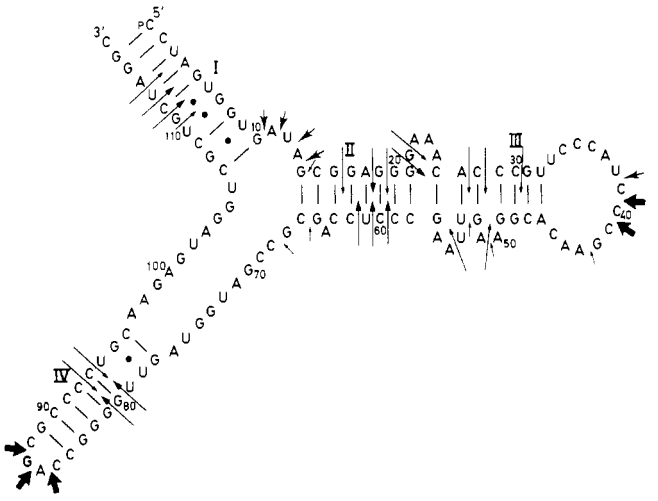

FIGURE 5: *B. stearothermophilus* 5S RNA drawn according to the Fox and Woese model with extensions to helices II and IV as drawn for the *E. coli RNA* in Figure 4. Arrows indicate the cutting positions of ribonucleases A, T_1, T_2, and cobra venom: the same system of arrows is used as for Figure 4.

& Garrett, 1979) was also based on comparative sequencing studies. All the data presented in this work are discussed with respect to this model.

Accessible Unpaired Nucleotides. The data for *E. coli* 5S RNA agree broadly with the earlier ribonuclease digestion studies of Monier and co-workers (Monier, 1974; Jordan, 1971; Vigne & Jordan, 1977) in that they reveal the three very accessible RNA regions C_{12} to U_{14}, U_{40} to C_{42}, and G_{86} to U_{89}. The data for the *B. stearothermophilus* 5S RNA show the corresponding accessible regions G_{10} to A_{13}, U_{38} to C_{40}, and C_{85} to G_{87} (see Figures 4 and 5). There is also evidence for other accessible regions previously undetected, namely, at C_{35}, C_{38}, A_{52}, and U_{65} in *E. coli* (Figure 4), although some ambiguity remains as to whether the cut at C_{38} is primary or secondary (see Table I). Only a weak cut occurs in the *B. stearothermophilus* RNA at A_{50}. We infer from this that the latter RNA is more highly structured than the *E. coli* RNA, and this inference is supported by the cobra venom ribonuclease results considered below. One negative result is of special interest, namely, the absence of a ribonuclease cut preceding A_{64}, the putative looped out base in the *B. stearothermophilus* RNA (Peattie et al., 1981; Garrett et al., 1981); this is the most reactive adenosine of both 5S RNAs to diethyl pyrocarbonate (Peattie et al., 1981; D. A. Peattie and R. A. Garrett, unpublished experiments; S. O. Olesen and R. A. Garrett, unpublished experiments). The relatively inaccessible C_{63}–A_{64} bond may, therefore, reflect the stable adjacent G–C base pairs in the *B. stearothermophilus* RNA.

Nucleotides which were previously inferred to be accessible in *E. coli* 5S RNA on the basis of ribonuclease cutting data, namely, G_{56} and C_{68} (Monier, 1974; Gray et al., 1973), are probably not accessible since the cut occurring at the former position is probably only seen in fragments and the latter is secondary. C_{68} was generally considered to be a primary cut because it is one of the two cuts which generates the highly ribonuclease resistant RNA fragment extending from G_{69} to C_{110} (Gray et al., 1973; Douthwaite et al., 1979). However, the present data reveal that the primary cut occurs at U_{65} and the sequence A_{66} to C_{68} is excised subsequently.

Double-Helical Regions. The cobra venom ribonuclease cuts provide the first experimental evidence for the double helices of the Fox and Woese model. Cuts were found in helices I, II, and IV of both *E. coli* and *B. stearothermophilus* 5S RNAs in approximately analogous positions, and these data are listed in Tables I and II and drawn in Figures 4 and 5. These double helices are also compatible with the absence of single-strand-specific ribonuclease cuts. No cobra venom ribonuclease cut was observed in the short helix III of the *E. coli* RNA and only a weak one was detected in the *B. stearothermophilus* RNA, but no primary single-strand cuts occurred in this helix either. The paucity of cobra venom ribonuclease cuts, and their presence in corresponding positions in the two RNAs, suggests that a special structural conformation is a prerequisite for their occurrence.

Although the cobra venom ribonuclease cuts occur on both sides of helices II and IV in Figures 4 and 5, the evidence from both 5′ and 3′ labeling shows, unambiguously, that the enzyme can approach from either side of the helix. There was no evidence that the enzyme cut right through the helix, and there was no reason, therefore, to conclude that the two halves of the molecules were maintained together after such a cut. It may be that the ribonuclease cannot cut right through the helix because the cuts through one strand will produce a certain flexibility in the complementary strand in that region, and this may inhibit the ribonuclease from cutting further if the ribonuclease substrate is a rigid helical structure.

No secondary cuts were observed for the cobra venom ribonuclease. This was surprising since it was expected that a cut in a helix might weaken interhelical interactions and lead directly to new cuts being produced. Conversely though, the absence of secondary cuts may reflect a paucity of interhelical interactions in the 5S RNA.

Other Highly Structured Regions. Long stretches of sequence are extremely unreactive in both RNA molecules to any of the single-strand-specific enzymes, namely, A_{15} to C_{35}, A_{53} to U_{65}, A_{66} to G_{86}, and C_{90} to U_{120} in *E. coli* and G_{14} to U_{38}, C_{41} to C_{85}, and C_{88} to C_{117} in *B. stearothermophilus*. One of these regions from C_{17} to G_{41} in *E. coli* was shown earlier by Jordan (1971) to be resistant to T_1 ribonuclease. These results demonstrate that the interhelical regions of the Fox and Woese model are highly structured, although there is little evidence for their forming regular double helices.

The loop regions 35–47 in *E. coli* and 33–45 in *B. stearothermophilus* 5S RNAs that also contain ribonuclease-resistant sequences C_{36} to A_{39} and U_{33} to A_{37}, respectively, are inaccessible, as is the highly conserved sequence C–G–A–A which was once proposed as a ribosomal binding site for tRNA (Forget & Weissman, 1967).

All of these ribonuclease-resistant regions strongly indicate the presence of extensive tertiary structural interactions in the RNAs, and this conclusion is supported by complementary chemical modification studies, on these two RNAs, using nucleotide-specific reagents (D. A. Peattie and R. A. Garrett, unpublished experiments; S. O. Olesen and R. A. Garrett, unpublished experiments). One such putative tertiary structural interaction was recently proposed between A_{24} and C_{39} in the *B. stearothermophilus* RNA on the basis of coordinated purine–pyrimidine and pyrimidine–purine changes at these two positions in Gram-positive bacteria (Studnicka et al., 1981), but it is not supported by the high degree of reactivity of C_{39} demonstrated here.

Differences between the Two RNA Structures. The general reactivity of the *B. stearothermophilus* 5S RNA appears to be lower than that of *E. coli*, suggesting a more stable structure. First, it was more resistant to breakdown during the renaturation procedure suggested by Weidner & Crothers (1977) (70 °C at 0.5 mM Mg^{2+}). Second, it was generally more resistant to single-strand-specific ribonuclease digestion; on average, more enzyme was required to produce the same

level of 5S RNA cutting as in *E. coli*. For example, the loop region U_{33} to C_{45} is decidedly less reactive in *B. stearothermophilus*. Moreover, the four-base loop (C_{85} – C_{88}) in *B. stearothermophilus* 5S RNA appears to confer extra stability on helix IV than the three-base loop found in *E. coli*; the four-base loop is a common feature of thermophilic bacteria.

The looped region between helices II and III of the Fox and Woese model (nucleotides 24–30 and 52–59 in *E. coli* and 22–28 and 50–57 in *B. stearothermophilus* 5S RNA) also exhibits some differences (Figures 4 and 5). One strong primary cut occurs in the former at A_{52}, whereas only a weak cut, at A_{50}, is seen in the latter RNA. Moreover, there are seven cobra venom ribonuclease cuts in this region of the latter and none in the *E. coli* RNA, thereby confirming the higher degree of structure in the *B. stearothermophilus* RNA.

Three base pairs, additional to those of the Fox and Woese model, are drawn in this region for both RNAs albeit in a slightly different configuration (Studnicka et al., 1981). In *E. coli* the base pairs are adjacent whereas in *B. stearothermophilus* only two are adjacent; the third constitutes an intercalated base pair C_{26}–G_{57}. This latter configuration does not fit the cobra venom ribonuclease data well since three of the cuts occur in single-stranded loop regions; the data would, however, be served better by the alternative intercalated base pair G_{22}–U_{54}.

Comparison with Chemical Modification Data and Alternative Models. Earlier chemical modification studies concentrated mainly on identifying the accessible nucleotides of *E. coli* 5S RNA to reagents specific for single-stranded regions such as carbodiimide, glyoxal, kethoxal, and methoxyamine [reviewed by Monier (1974)]. These studies served mainly to demonstrate the accessibility of G_{13}, G_{41}, U_{40}, U_{85}, and U_{87}. More recently, a kinetic study on the A conformer of *E. coli* 5S RNA with kethoxal (Noller & Garrett, 1979) revealed that G_{13}, G_{24}, G_{41}, and G_{69} were rapidly modified whereas G_{16}, G_{23}, G_{44}, G_{86}, and G_{107} reacted slowly. These results are included in Figure 4 with large and small K's, respectively. The guanines in the latter group appear to occur in the relatively unstable structured regions, for example, at the ends of helices.

In parallel studies, we have recently investigated the chemical accessibilities of the guanine, adenine, and cytosine residues of both *E. coli* and *B. stearothermophilus* 5S RNAs to dimethyl sulfate and diethyl pyrocarbonate (D. A. Peattie and R. A. Garrett, unpublished experiments). These modification data correlate with the ribonuclease cuts in that they tend to occur at the same accessible, unpaired nucleotides. Of special interest is the looped out adenine drawn in helix II which is strongly modified in both RNAs (Peattie et al., 1981; S. O. Olesen and R. A. Garrett, unpublished experiments) and also the region between helices II and III. The data are compatible with the proposed structures of Studnicka et al. (1981) drawn in Figures 4 and 5 in that mainly looped out bases are modified. For example, in *E. coli* 5S RNA, in Figure 4, G_{24}, C_{26}, C_{27}, A_{52}, A_{53}, and A_{59} are modified. This would suggest that the other looped out bases in this region are involved in tertiary interactions of some kind. However, it is probably too early to draw any definite conclusions about the structure of this region.

A large number of alternative base-pairing schemes have been offered, especially for *E. coli* 5S RNA [reviewed by Erdmann (1976)]. While most of these have certain common features, in particular helices I and IV, they do not stand the important test of comparative sequence studies for the rest of the structure. One model, however, consisting of a cloverleaf structure (Luoma & Marshall, 1978) was claimed by the authors to fit most of the published experimental data. This model contains extended versions of helices I and III and helix IV of the Fox and Woese model but dispenses with helix II and forms an alternative base-paired structure in the sequence 63–82. The present data are incompatible with this change chiefly because the strong cobra venom ribonuclease cuts which are drawn on the upper side of helix II in Figures 4 and 5 fall in single-stranded regions in the cloverleaf model.

This work which was performed on the native conformer of 5S RNA in ribosomal reconstitution buffer has provided a basis for studies on protein binding sites on the 5S RNAs which will be presented in a subsequent paper (S. Douthwaite et al., unpublished experiments).

Acknowledgments

Anni Christensen is thanked for her excellent assistance with some experiments. We appreciate the generous provision of the cobra venom ribonuclease by A. S. Butorin and S. Vassilenko.

References

Dohme, F., & Nierhaus, K. H. (1976) *Proc. Natl. Acad. Sci. U.S.A. 73*, 2221–2225.

Douthwaite, S., Garrett, R. A., Wagner, R., & Feunteun, J. (1979) *Nucleic Acids Res. 6*, 2453–2470.

Erdmann, V. A. (1976) *Prog. Nucleic Acid Res. Mol. Biol. 18*, 45–90.

Forget, B., & Weissman, S. M. (1967) *Science (Washington, D.C.) 158*, 1695–1699.

Fox, G. E., & Woese, C. (1975) *Nature (London) 256*, 505–507.

Garrett, R. A., Douthwaite, S., & Noller, H. F. (1981) *Trends Biochem. Sci. (Pers. Ed.) 6*, 137–139.

Gray, P. N., Bellemare, G., Monier, R., Garrett, R. A., & Stöffler, G. (1973) *J. Mol. Biol. 77*, 133–152.

Jordan, B. R. (1971) *J. Mol. Biol. 55*, 423–439.

Luoma, G. A., & Marshall, A. G. (1978) *Proc. Natl. Acad. Sci. U.S.A. 75*, 4901–4905.

Monier, R. (1974) in *Ribosomes* (Nomura, M., Tissières, A., & Lengyel, P., Eds.) pp 141–168, Cold Spring Harbor Laboratory, Cold Spring Harbor, NY.

Monier, R., & Feunteun, J. (1971) *Methods Enzymol. 20*, 494–502.

Noller, H. F., & Garrett, R. A. (1979) *J. Mol. Biol. 132*, 621–636.

Peattie, D. A. (1979) *Proc. Natl. Acad. Sci. U.S.A. 76*, 1760–1764.

Peattie, D. A., Douthwaite, S., Garrett, R. A., & Noller, H. F. (1981) *Proc. Natl. Acad. Sci. U.S.A.* (in press).

Stanley, J. R., & Penswick, J. R. (1975) *Proc. FEBS Meet., 9th*, Abstr. 421.

Stöffler, G., Bald, R., Kastner, B., Lührmann, R., Stoffler-Meilicke, M., & Tischendorf, G. (1980) in *Ribosomes* (Chamblis G., et al., Eds.) pp 171–205, University Park Press, Baltimore, MD.

Studnicka, G M., Eiserling, F. A., & Lake, J. A. (1981) *Nucleic Acids Res. 9*, 1885–1904.

Vassilenko, S., & Babkina, V. (1965) *Biokhimiya 30*, 705–712.

Vigne, R., & Jordan, B. R. (1977) *J. Mol. Evol. 10*, 77–86.

Weidner, H., & Crothers, D. M. (1977) *Nucleic Acids Res. 4*, 3401–3414.